International Journal of Power Electronics and Drive System (IJPEDS)
Vol. 17, No. 2, June 2026, pp. 1396~1407
ISSN: 2088-8694, DOI: 10.11591/ijpeds.v17.i2.pp1396-1407

Control strategy for the combined operation of grid-connected inverter and charger

Quang-Tho Tran, Quang-Sang Le
Faculty of Electrical and Electronics Engineering, HCM City University of Technology and Engineering, Ho Chi Minh City, Vietnam

Article Info

Article history:

Received Oct 28, 2025
Revised Feb 24, 2026
Accepted Mar 6, 2026

Keywords:

Battery charger
Combined control
Constant current
Constant voltage
Dual active converter
Grid-connected inverter

ABSTRACT

Solar power sources and electric vehicles (EVs) are increasingly used because of their environmental friendliness and sustainability. They are typically connected to the power grid through devices such as inverters and chargers to either generate or receive electrical energy. These devices contain a DC voltage bus. Therefore, the combined control of these two types of devices can improve their overall operational efficiency. This article proposes a grid-connected converter with an integrated battery-charging function. In addition, it presents a control strategy for the coordinated operation of this converter during both charging and power generation at the DC bus. In this algorithm, the battery is treated as a priority load, which allows the system to eliminate the AC–DC converter used in conventional chargers. A total peak power of 9 kWp is used to investigate the processes of power generation and battery charging. The total harmonic distortions of grid current are less than 2.86% in different operational cases and meet the grid codes. The obtained results are analyzed under varying irradiance conditions to verify the effectiveness of the proposed control method.

Corresponding Author:

Quang-Tho Tran
Faculty of Electrical and Electronics Engineering, HCM City University of Technology and Engineering
Ho Chi Minh City, Vietnam
Email: thotq@hcmute.edu.vn

1. INTRODUCTION

In recent years, along with the global shift toward green energy, single-phase grid-connected inverters used in rooftop photovoltaic (PV) systems have become increasingly popular around the world [1]-[6]. Households and small businesses install these systems to take advantage of the abundant solar energy, reduce electricity costs, and contribute to environmental protection [7], [8]. The inverter plays a crucial role in converting direct current (DC) generated by solar panels into alternating current (AC) [9] that is synchronized with the utility grid, allowing power to be fed into the grid, supplied to local loads, or even sold back to the electricity provider [8]. At the same time, the rapid development of electric vehicles (EVs) has driven a growing demand for smart battery chargers [10], [11]. Charging stations, from residential to public ones, are being widely deployed to support the transition to electric mobility. An electric vehicle (EV) charger converts grid power into a stable DC to charge the vehicle's battery and integrates protection, monitoring, and communication functions into the energy management system [12], [13].

Notably, the circuit structures of grid-connected inverters and EV battery chargers share many similarities. Both are based on DC/DC and DC/AC power conversion stages that utilize high-power semiconductor devices such as IGBTs or MOSFETs, combined with filtering circuits and digital control systems. In many current studies, researchers are aiming to integrate these two devices into a single hybrid structure [14]-[17], which can perform both grid connection and battery charging functions, thereby

optimizing energy utilization efficiency and reducing investment costs for future smart power systems [18]-[21]. Most of the control methods of these devices in [8], [22]-[30] essentially focus on the control of chargers and consider the effect of irradiance on power quality [30]. The technique in [31] presented on hybrid PV-grid systems with inverters for EV charging, emphasizing control strategies like maximum power point tracking (MPPT) and pulse-width modulation (PWM). The strategies in [32], [33] used the 3-phase grid sources to charge the battery. In addition, the method in [34] integrated PV and wind into a DC smart grid for EV/PHEV charging via ring topology and hybrid multilevel inverters. In the meantime, the single-phase grid-connected inverters used in rooftop PV systems have become increasingly common in residential applications. The single-phase battery charging and grid-connected systems have not yet been comprehensively investigated or analyzed to develop effective control strategies. Moreover, the reactive power generation to support the grid has also not been comprehensively considered.

Therefore, this article introduces a grid-connected converter equipped with an integrated battery-charging capability. It also proposes a control strategy that enables coordinated operation of the converter during both energy generation and battery charging through the DC bus. In the proposed approach, the battery is treated as a priority load, allowing the system to eliminate the separate AC–DC conversion stage commonly used in traditional chargers. The DC bus voltage is boosted from the solar panels and directed to charge the battery via a dual active bridge (DAB) configuration. Meanwhile, the grid-connected inverter utilizes the same DC bus to regulate power generation or absorption from the grid, ensuring efficient and unified system operation. Thus, the novelty and contribution of this article are a recommendation to the manufacturers of grid-connected inverters on the integration of the battery charging function and the battery treatment as a priority load. This helps remove the rectifier and booster from the charger. Then, the effective control and operation of these systems will open up avenues for future research. The structures of the grid-connected inverter and battery charger are shown in section 2. The proposed system structure using the DC point of common coupling is presented in section 3, and the strategy of combined control is presented in detail in this section. Section 4 shows the investigated results in cases of changes of irradiance conditions and the process of battery charging. Additionally, the results are also discussed and analyzed in detail. Section 5 presents the advantages of the proposed structure and control strategy.

2. GRID-CONNECTED CONVERTERS

In the conventional converters, the grid-connected inverter is used to generate the active power from the solar panels into the grid, while the charger is used to convert the active power from the grid to charge the vehicle's battery. Though both connect to the power grid, they independently operate. The following is their structure.

2.1. Grid-connected inverter structure using solar panels

A single-phase grid-connected solar inverter system, shown in Figure 1, integrates solar array, a DC-DC booster to optimizes the power from the solar array via MPPT, an inverter to convert DC to grid-compatible AC, filtering circuit to ensure clean output, a control system including a DC voltage controller and a current controller, a grid interface to enable safe grid connection through a phase-locked loop (PLL), and a DC voltage bus. These components work together to deliver efficient, stable, and safe power from solar energy to the grid, supporting renewable energy adoption.

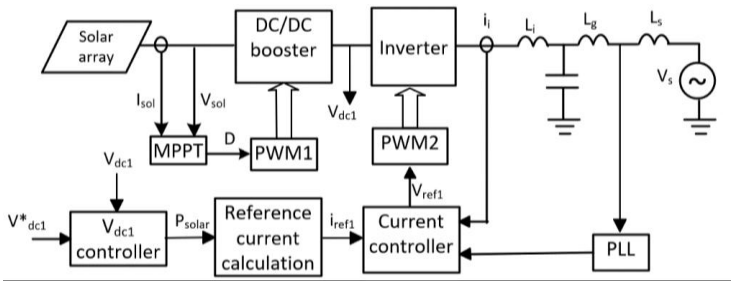

Figure 1. Single-phase grid-connected solar inverter system

2.2. Battery charger structure

In residential areas, the battery charging converters conventionally consist of the basic blocks as shown in Figure 2. Where a rectifier is used to convert the power from the grid into DC power, and a

converter to boost the DC voltage up to 400 V with a function of power factor correction (PFC). In addition, a DAB converter is used to charge the battery via a high-frequency isolation transformer.

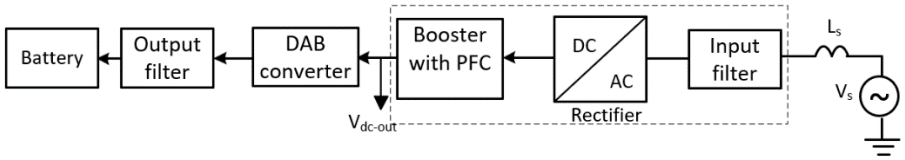

Figure 2. Structure of a battery charger using a single-phase grid

3. PROPOSED CONTROL STRATEGY

In section 2, Figures 1 and 2 show that both the grid-connected inverter and battery charger contain a DC voltage bus. The voltage of these DC buses is about 400 V. Therefore, the combination of these two devices helps remove the components, surrounded by the dashed line, from the charger in Figure 2, such as the booster with PFC, rectifier, and input filter. Besides removing the hardware from the charger, the controllers for these components also reduce the burden of computation. Thus, this paper proposes a structure as shown in Figure 3(a). The main circuit of the inverter is shown in Figure 3(b), and the impulses from the PWM2 generator use the unipolar modulation technique as shown in Figure 3(c). In this system, a grid-connected inverter using a solar array with the function of battery charging is used to generate the active and reactive powers into the grid. When a battery is connected to the system, it is treated as a priority load, whether the power of the solar array is high or low.

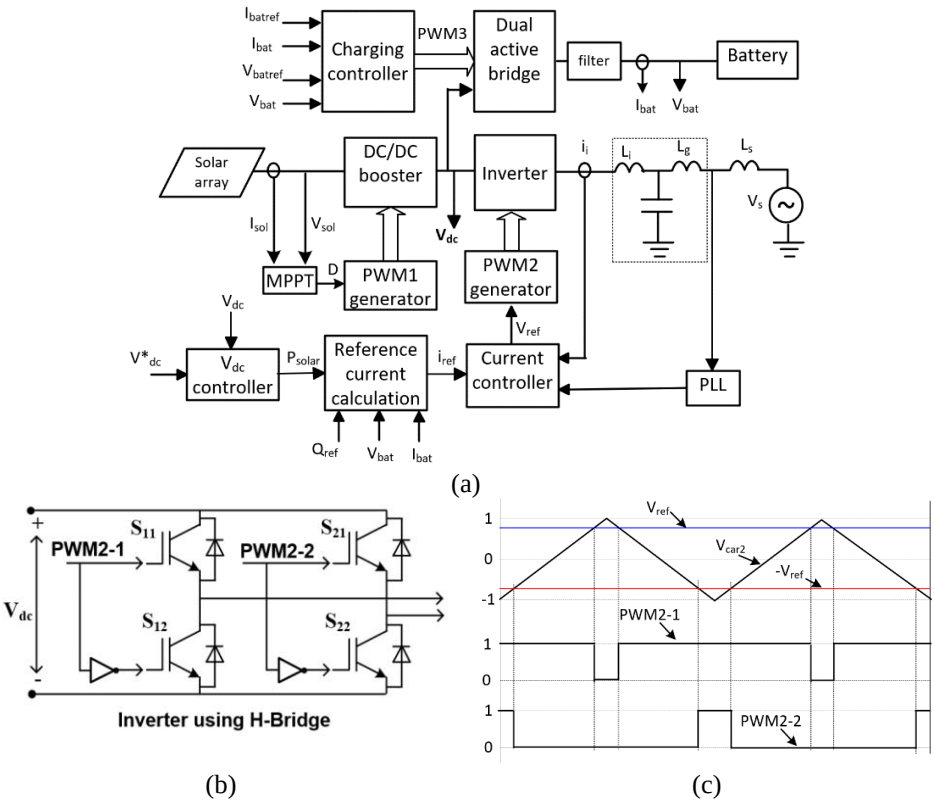

Figure 3. Proposed system: (a) structure of the system, (b) main circuit of the inverter, and (c) PWM2 generator

3.1. Control of battery charger

To control the charger current and voltage, a DC/DC converter uses two active H-bridges as shown in Figure 4(a). To ensure safety at the charger output side, the DAB converter has its input and output

isolated from each other through a high-frequency transformer with a 1:1 turn-down ratio. Where Lr is the primary side resonant filter inductance. The impulses for these two H-bridges have the same switching frequency f_{sw} and 50% pulse width.

The power transmitted from the primary side input with voltage V_{pr} to the secondary side output with voltage V_{se} is adjusted by the method of shifting the secondary side impulse. The impulses for the primary side H-bridge transistors with the symbol G_{fix} have a fixed phase. The impulses for the secondary side H-bridge transistors with the symbol G_{shi} use the method of shifting the phase with a 50% pulse width $G_{fix1} = G_{fix}$; G_{fix2} = inverse of G_{fix}; $G_{shi1} = G_{shi}$; G_{shi2} = inverse of G_{shi}. Then, the power transmitted through the converter is determined as (1).

$$P = \frac{V_{pr} * V_{se}}{X_{Lr}} sin\,\alpha \quad (1)$$

Where α is the phase-shifted angle between the impulses of G_{fix} and G_{shi}. The primary and secondary voltages are as (2) and (3). Then, the power can be deduced from (1)-(3) as (4). The current and voltage regulation of the charger can also be defined as (5) and (6) based on the small signal model with the constants C_v and C_i through the derivatives of voltage ΔV_{bat}, current ΔI_{bat}, and phase-shifted angle $\Delta\alpha$. The impulse generation principle is also shown in Figure 4(b).

$$V_{se} = \frac{4 * V_{bat}}{\pi\sqrt{2}} \quad (2)$$

$$V_{pr} = \frac{4 * V_{dc}}{\pi\sqrt{2}} \quad (3)$$

$$P = \frac{8 * V_{dc} * V_{bat}}{\pi^2 * X_{Lr}} sin\,\alpha \quad (4)$$

$$\Delta V_{bat} \approx C_V * \Delta\alpha \quad (5)$$

$$\Delta I_{bat} \approx C_I * \Delta\alpha \quad (6)$$

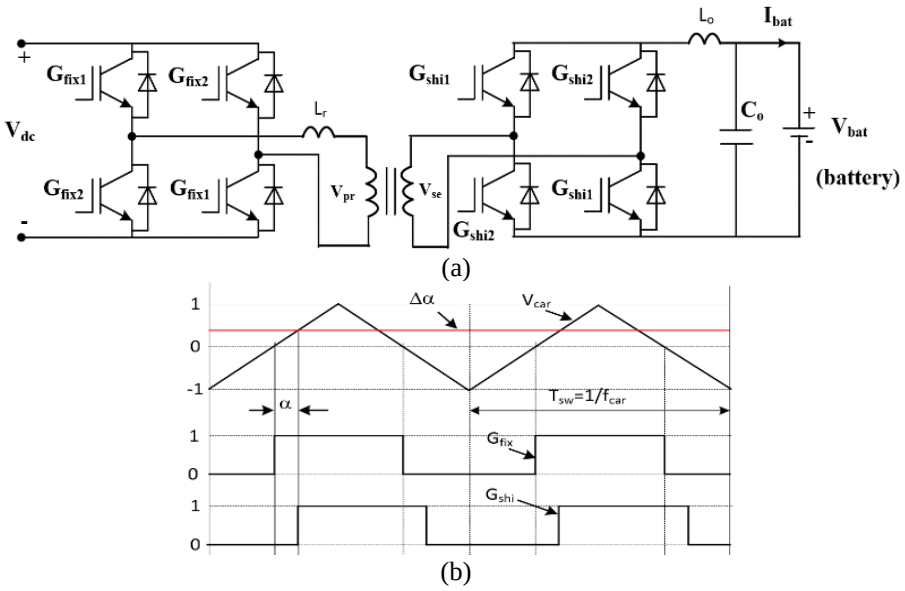

Figure 4. Dual active bridge and generation of impulses: (a) DAB and (b) principle of impulse generation

The EVs commonly run on lithium-ion batteries. This type is charged in two stages. In the first stage, the constant current (CC) control is used, and the second one uses the constant voltage (CV) control to charge, as shown in Figure 5(a). When the charging current decreases small enough, the trickle current, the system stops charging the battery. The control principle is also presented in Figure 5(b). Where K_{pv} and K_{iv} are the coefficients of the PI controller in the CV control mode. The K_{pi} and K_{ii} are the coefficients of the PI controller in the CC control.

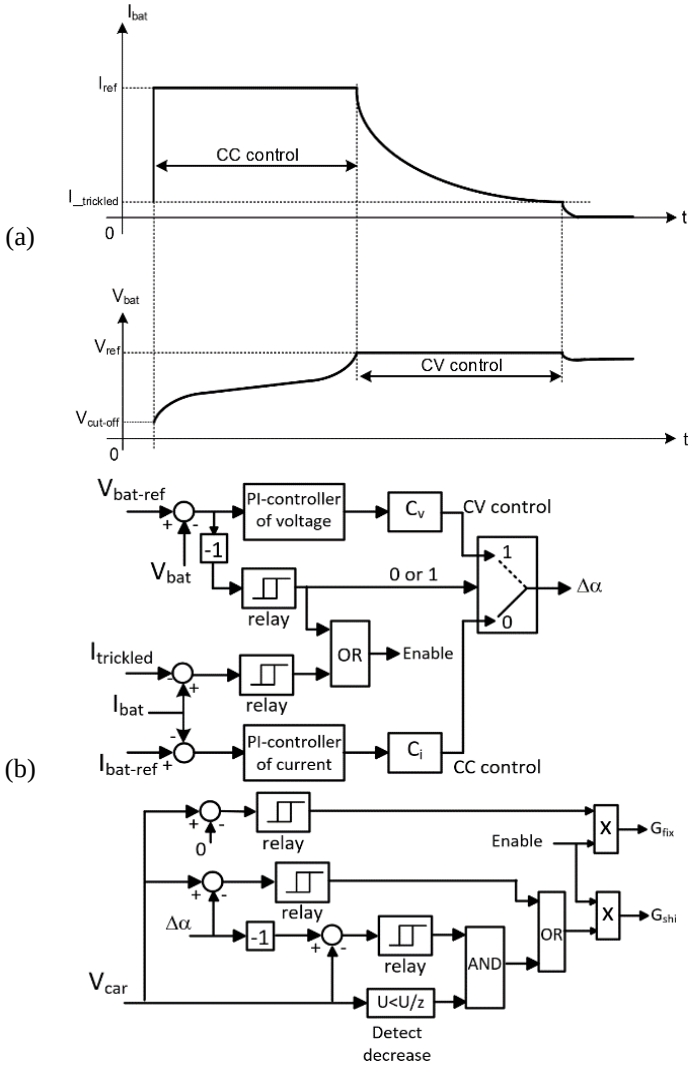

Figure 5. Control principle of charger: (a) charging characteristics and (b) principal diagram of charging controllers in MATLAB/Simulink

3.2. Control of grid-connected converter system

In Figure 3, the PLL block is used to estimate the parameters of the grid voltage, such as the magnitude Vmax, angular frequency ω0, and phase angle θ, to synchronize the system with the grid. The control principal diagram of the grid-connected converter is also shown in Figure 6. The voltage quantities, Va and Vb, are defined as (7) and (8).

$$V_\alpha = V_{max} \quad sin\,\theta \tag{7}$$

$$V_\beta = V_{max} \quad cos\,\theta \tag{8}$$

The voltage of DC bus is regulated as Vdc-ref by the PI controller. This voltage is also the DC input of the charger in Figure 4(a). Then, the optimum power is extracted from the solar array as Psolar via an algorithm of MPPT. At the same time, the power used to charge the battery Pbat is also defined as (9). Where V_{bat} and I_{bat} are the voltage and current measured at the output of the charger in Figure 4(a).

$$P_{bat} = V_{bat} * I_{bat} \tag{9}$$

$$P_{ref} = P_{solar} - P_{bat} \tag{10}$$

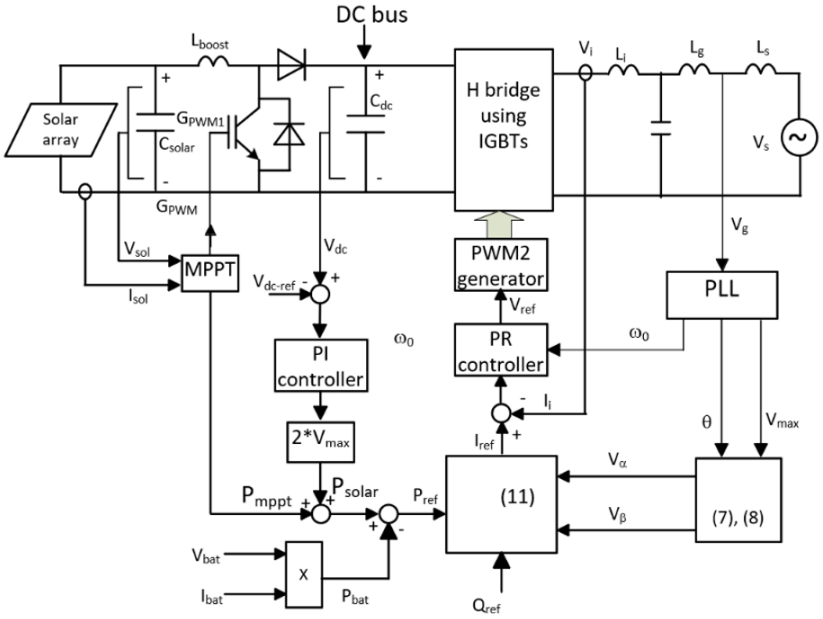

Figure 6. Grid-connected converter system

As mentioned above, the battery is considered the priority load. Therefore, every time the battery is connected to the charger, the battery is charged from the solar array or/and/or the grid. Then, the reference active power of the inverter is P_{ref} and defined as (10). In case the power extracted from the solar array is smaller than the charging power of the battery, the reference power P_{ref} is negative, and the inverter is operated as a rectifier to consume the power from the grid for charging the battery.

$$I_{ref} = 2\left(\frac{V_\alpha * P_{ref} - V_\beta * Q_{ref}}{V_\alpha^2 + V_\beta^2}\right) \quad (11)$$

The reference current of the inverter generating into the grid is calculated as (11) based on the reference reactive and active powers, Q_{ref} and P_{ref}, and the voltages, V_α and V_β, to synchronize with the grid. This current is regulated by the proportional resonance (PR) controller with the transfer function as (12). Where ω_0 is the angular frequency of the grid voltage estimated by the PLL.

$$H(s) = K_{pi} + K_{ir}\frac{s}{s^2 + \omega_0^2} \quad (12)$$

4. RESULTS AND DISCUSSION

The system parameters are shown in Table 1 and simulated on MATLAB/Simulink. In this system, an algorithm of incremental conductance is used for the MPPT block with the change of irradiance, as shown in Figure 7. The simulation results are also shown in Figures 8-17. The irradiance values vary from 0 to 1 (1 is as 1000 W/m^2) in many different intervals of time from 0 to 40 s. The DC bus voltage is regulated to 400 V in Figure 8(a), regardless of the change in irradiance. The responses of the solar array voltage and current are shown in Figures 8(a) and 8(b). The extracted power is also shown in Figure 8(c) by the MPPT.

The reference reactive power Q_{ref} is stepped from 0 down to -2.5 kVar (consuming from the grid) at a time of 1.5 s. Then, at the time at 8.5 s, the Q_{ref} is stepped up to 2.5 kVar (generating into the grid). The active power of the inverter is generated into the grid or consumed from the grid depending on the battery status, charging power, and irradiance.

Table 1. System parameters

Description	Symbol	Value	Description	Symbol	Value
Grid voltage	V_g	220 VAC	DC voltage controller coefficients	k_{pdc}; k_{idc}	0.3; 2
Grid frequency	f_g	50 Hz	PR current controller	k_{pi}; k_{ir}	46.2; 5712
Total power of the solar array	P_{solar}	9157 Wp	PI controller's coefficients of CC and CV	k_p; k_i	0.01; 0.1
Battery lithium-ion capacitor	C_{bat}	4.32 Ah	Switching frequency of DAB	f_{car}	2 kHz
Initial state of charge (SOC)	SoC	30%	Switching frequency of the converter	f_{sw}	10 kHz

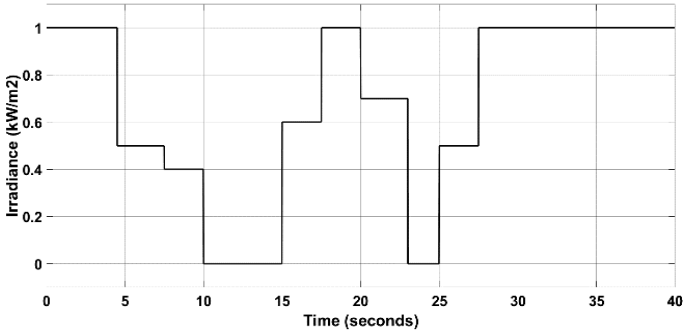

Figure 7. Irradiance changes of the solar array

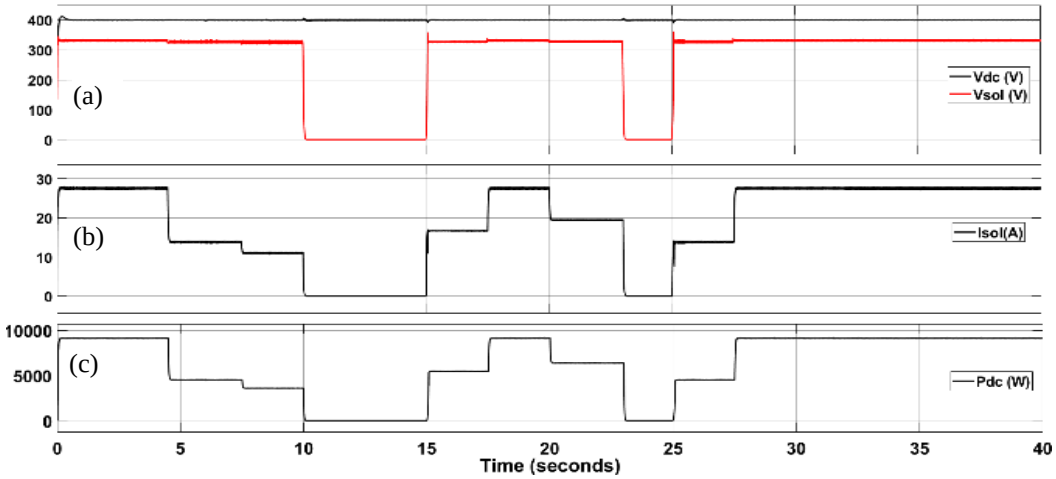

Figure 8. Solar array responses: (a) DC bus voltage and solar array voltage, (b) current, and (c) power

The reference charging voltage $V_{bat\text{-}ref}$ is set as 275 V while the reference charging current $I_{bat\text{-}ref}$ varies according to the steps, in the interval of 0-3 s as 20 A, in 3-6 s as 25 A, and from 6 s to the remaining of the charging progress in CC control stage as 35 A. The voltage and current responses of the charging process are shown in Figures 9(a) and 9(b). The charger firstly operates in the CC control stage with different reference currents. However, at the time 11.5 s, the battery voltage increases up to the reference voltage of 275 V, and the charger is switched to operate in the CV control stage. The SOC response of the battery is also shown in Figure 10.

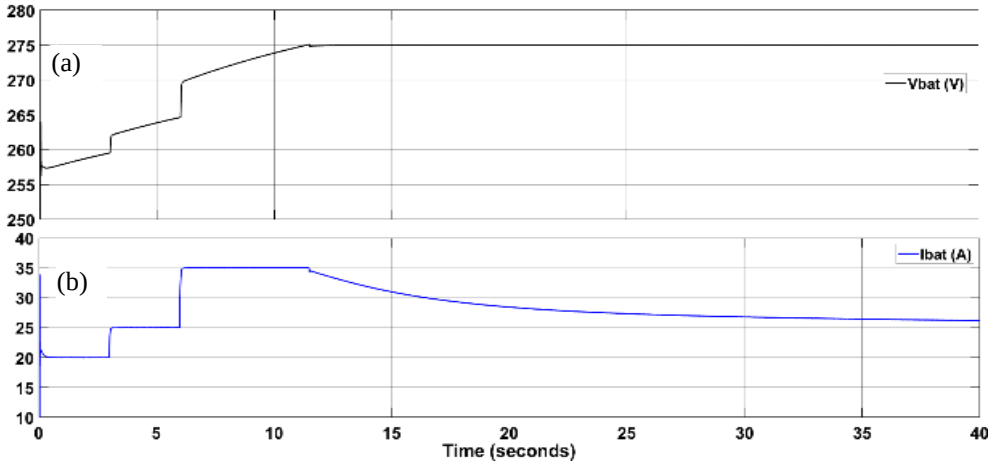

Figure 9. Battery charging voltage and current: (a) charging voltage and (b) charging current

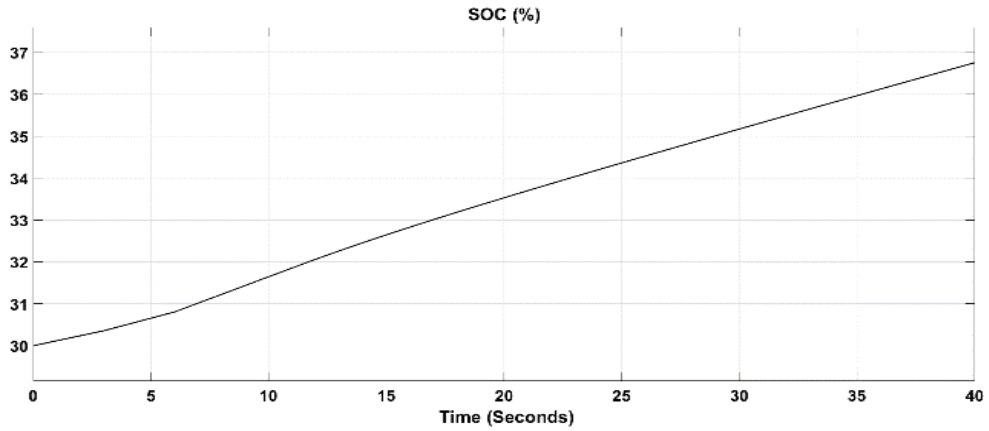

Figure 10. SOC response of the battery

In case the battery has not been plugged into the charger, the responses of power are shown in Figure 11. Then, the inverter generates the power into the grid, P_g in the red line, approximately as the power of the solar array, P_{solar} in the green line. While the charging power is zero, P_{bat} is in the black line. Thus, the system operates as a normal grid-connected inverter.

On the contrary, in Figure 12, when the battery is plugged into the charger, the charging power P_{bat} in the black line varies during the charging process with different values, respectively, with the change of the reference charging current values. In the intervals of 0-4.5 s, 17.5-20 s, and 27.5-40 s, the solar array power P_{solar} is greater than the charging power P_{bat}, the charger is supplied with some power of solar array. The redundant power of the solar array, the positive power P_g in the red line, is generated into the grid by the inverter. However, in the intervals of 4.5-17.5 s and 20-27.5 s, the solar power P_{solar} is lower than the charging power P_{bat}, then, the system switches to operate as a rectifier to consume some power from the grid, negative values P_g in the red line, to supply the charger.

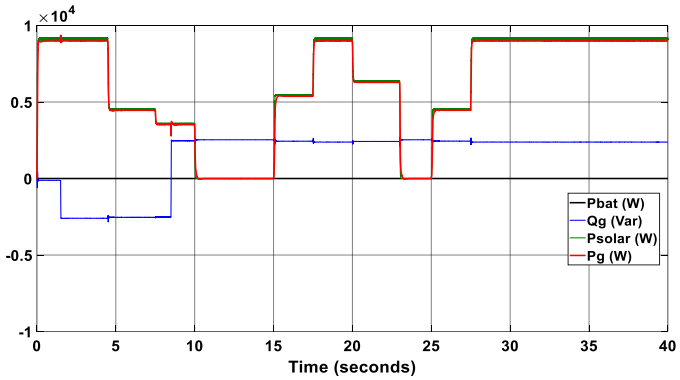

Figure 11. Power responses without a battery

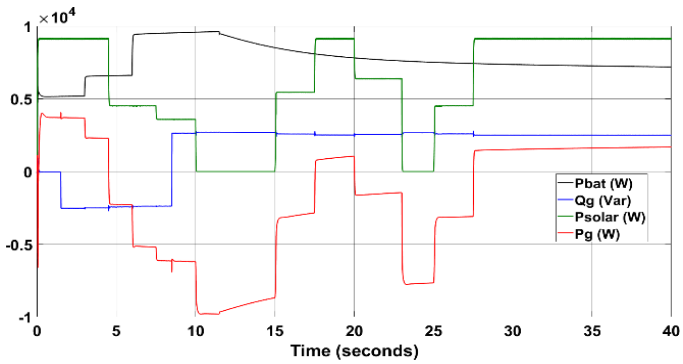

Figure 12. Power responses with battery charging

The waveforms of grid voltage and current of the two cases, with and without a battery, are shown in Figures 13 and 14. Figures 15 and 16 present the zoomed-in waveforms of grid voltage and current for the two cases, without and with battery charging, respectively. The waveforms of grid voltage in Figures 13(a) and 14(a) are similar for both cases, with and without a battery plugged in. These waveforms are also zoomed in 1.48-1.54 s in Figures 15(a) and 16(a), respectively. Because the short-circuit apparent power of the grid is very high. However, the waveform of grid current in Figure 13(b) is different from that in Figure 14(b). The grid current magnitudes zoomed, in Figures 15(b) and 16(b), before the time 1.5 s, are lower than those after the time 1.5 s because the system only generates the active power into the grid. After 1.5 s, the system generates the active power and consumes the reactive power. However, the operational progress smoothly switching has shown the effectiveness of the proposed control strategy. Moreover, the values of current total harmonic distortion (THD) in Figures 17(a) and 17(b) of both cases, measured in one fundamental period from 14.98 s and 19.98 s, respectively, are 2.86% and 2.81% in the intervals with the lowest grid current magnitudes.

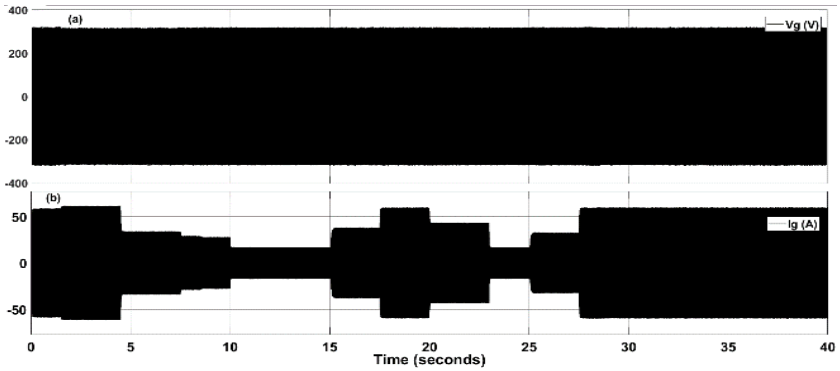

Figure 13. Grid voltage and current without battery: (a) voltage and (b) current

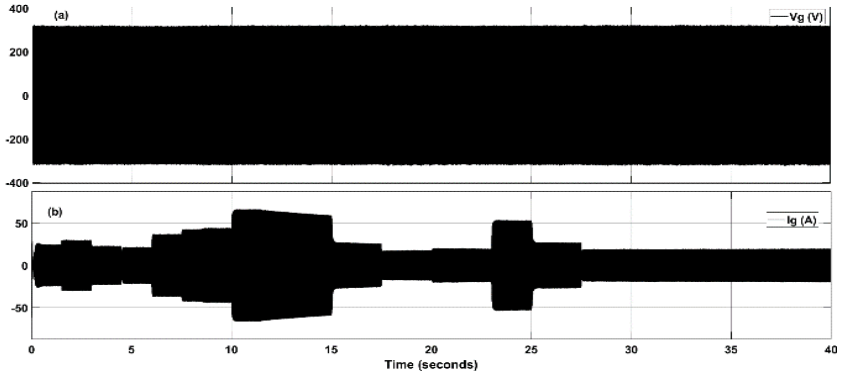

Figure 14. Grid voltage and current with battery: (a) voltage and (b) current

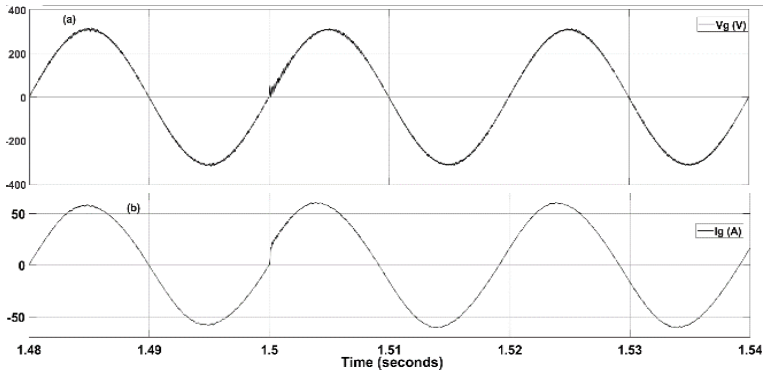

Figure 15. Waveforms of grid voltage and current zoomed in 1.48-1.54 s without battery charging: (a) grid voltage and (b) grid current

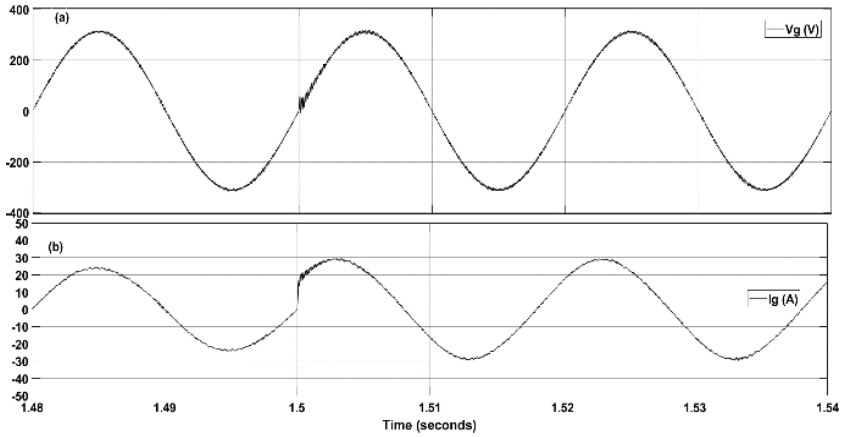

Figure 16. Waveforms of grid voltage and current in 1.48-1.54 s with battery charging: (a) grid voltage and (b) grid current

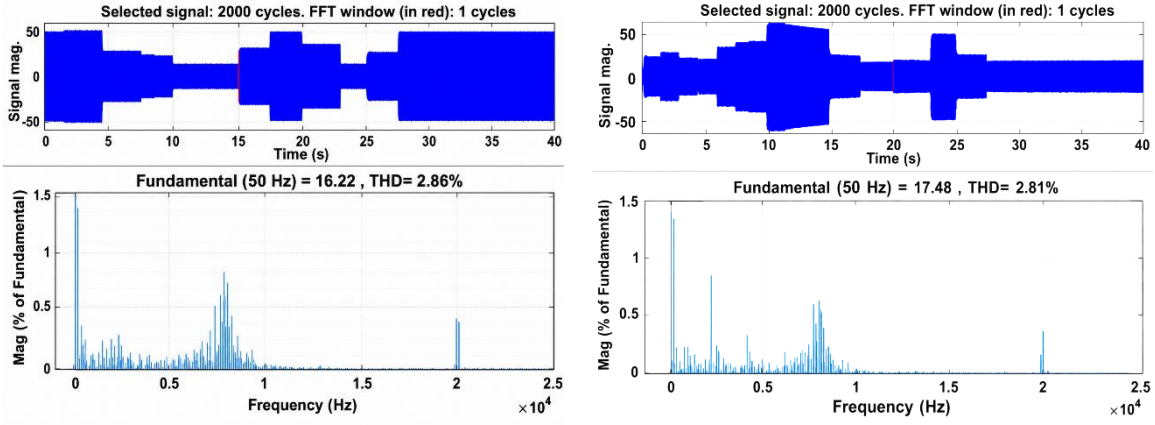

(a) (b)

Figure 17. Harmonic spectrum of grid current: (a) without battery charging and (b) with battery charging

5. CONCLUSION

The combined control method presented in this system offers the functions of both a charger and a grid-connected inverter using solar panels. In the proposed structure, the boost converter with PFC, rectifier, and input filter of the conventional battery charger are completely removed. The power to charge the battery is supplied from a solar array and/or the grid, depending on the change of irradiance and battery charging progress. The simulation results have validated the effective operation of the system through the responses of powers, voltages, currents, and the battery parameters in the charging stages of CC and CV control. Additionally, the grid current THD values are also lower than 2.86% and completely meet the grid codes. The simulation results are also considered and analyzed quantitatively in both cases, with and without battery charging. This structure offers expansive applications such as battery energy storage system (BESS), vehicle to grid (V2G), or grid to vehicle (G2V) in urban areas. Then, the power quality improvements of these systems in the charging process will open up avenues for future research.

ACKNOWLEDGMENTS

This work belongs to the project T2025-213 funded by Ho Chi Minh City University of Technology and Engineering, Vietnam.

FUNDING INFORMATION

Authors state no funding involved.

AUTHOR CONTRIBUTIONS STATEMENT

This journal uses the Contributor Roles Taxonomy (CRediT) to recognize individual author contributions, reduce authorship disputes, and facilitate collaboration.

Name of Author	C	M	So	Va	Fo	I	R	D	O	E	Vi	Su	P	Fu
Quang-Tho Tran	✓	✓	✓	✓	✓	✓		✓	✓	✓		✓	✓	✓
Quang-Sang Le						✓	✓	✓		✓	✓			✓

C : **C**onceptualization
M : **M**ethodology
So : **So**ftware
Va : **Va**lidation
Fo : **Fo**rmal analysis
I : **I**nvestigation
R : **R**esources
D : **D**ata Curation
O : Writing - **O**riginal Draft
E : Writing - Review & **E**diting
Vi : **Vi**sualization
Su : **Su**pervision
P : **P**roject administration
Fu : **Fu**nding acquisition

CONFLICT OF INTEREST STATEMENT

The authors state no conflict of interest.

DATA AVAILABILITY

The data that support the findings of this study are available from the corresponding author, [QT], upon reasonable request.

REFERENCES

[1] B. K. Santhoshi, K. M. Sundaram, S. Padmanaban, J. B. Holm-Nielsen, and K. K. Prabhakaran, "Critical review of PV grid-tied inverters," *Energies*, vol. 12, no. 10, 2019, doi: 10.3390/en12101921.

[2] M. Y. A. Khan, H. Liu, Z. Yang, and X. Yuan, "A comprehensive review on grid connected photovoltaic inverters, their modulation techniques, and control strategies," *Energies*, vol. 13, no. 6, 2020, doi: 10.3390/en13164185.

[3] S. Deshpande and N. R. Bhasme, "A review of topologies of inverter for grid-connected PV systems," in *2017 Innovations in Power and Advanced Computing Technologies, i-PACT 2017*, 2017, pp. 1–6. doi: 10.1109/IPACT.2017.8245191.

[4] I. Jamal, M. F. Elmorshedy, S. M. Dabour, E. M. Rashad, W. Xu, and D. J. Almakhles, "A comprehensive review of grid-connected pv systems based on impedance source inverter," *IEEE Access*, vol. 10, pp. 89101–89123, 2022, doi: 10.1109/ACCESS.2022.3200681.

[5] E. Kabalcı, "Review on novel single-phase grid-connected solar inverters: circuits and control methods," *Solar Energy*, vol. 198, pp. 247–274, 2020, doi: 10.1016/j.solener.2020.01.063.

[6] M. Morey, N. Gupta, M. M. Garg, and A. Kumar, "A comprehensive review of grid-connected solar photovoltaic system: architecture, control, and ancillary services," *Renewable Energy Focus*, vol. 45, pp. 307–330, 2023, doi: 10.1016/j.ref.2023.04.009.

[7] D. Selvaraj and D. Rangasamy, "Roof top pv for charging the ev using hybrid GWO-CSA," *International Journal of Power Electronics and Drive Systems*, vol. 13, no. 2, pp. 1186–1194, 2022, doi: 10.11591/ijpeds.v13.i2.pp1186-1194.

[8] J. Srivichai, K. Somsai, and N. Pornsuwancharoen, "Modeling and analysis of three-phase boost rectifier for DC fast EV charging," *International Journal of Power Electronics and Drive Systems*, vol. 16, no. 2, pp. 1094–1106, 2025, doi: 10.11591/ijpeds.v16.i2.pp1094-1106.

[9] F. Han, X. Zhang, and M. Li, "Hybrid-mode control for grid-connected inverters and characteristics comparison with current-source mode and voltage-source mode," *International Journal of Electrical Power & Energy Systems*, vol. 170, p. 110911, Sep. 2025, doi: 10.1016/j.ijepes.2025.110911.

[10] H.-S. Kang, S.-M. Kim, Y. Bak, and K.-B. Lee, "A controller design for a stability improvement of an integrated charging system in hybrid electric vehicle," *IFAC-PapersOnLine*, vol. 52, no. 4, pp. 141–146, 2019, doi: 10.1016/j.ifacol.2019.08.169.

[11] L. Sun, X. Wang, and C. Ma, "Bidirectional power control strategy for on-board charger based on single-stage three-phase converter," *Electronics*, vol. 13, no. 6, p. 1041, Mar. 2024, doi: 10.3390/electronics13061041.

[12] D. Mishra, S. Mandal, A. Darcy Gnana Jegha, T. Thangam, M. Antony Freeda Rani, and D. Karthikeyan, "Firefly-optimized energy management with improved boost converter for hybrid charging of electric vehicles," in *International Conference on Power Electronics and Renewable Energy Systems*, 2026, pp. 313–324. doi: 10.1007/978-981-95-0207-3_28.

[13] R. Xiong, Q. Yu, and L. Y. Wang, "Open circuit voltage and state of charge online estimation for lithium ion batteries," *Energy Procedia*, vol. 142, pp. 1902–1907, Dec. 2017, doi: 10.1016/j.egypro.2017.12.388.

[14] M. Quraan, M. Abu-Khaizaran, J. Sa'ed, W. Hashlamoun, and P. Tricoli, "Design and control of battery charger for electric vehicles using modular multilevel converters," *IET Power Electronics*, vol. 14, no. 1, pp. 140–157, Jan. 2021, doi: 10.1049/pel2.12018.

[15] F. Nasr Esfahani, A. Darwish, and X. Ma, "Design and control of a modular integrated on-board battery charger for EV applications with cell balancing," *Batteries*, vol. 10, no. 1, p. 17, Jan. 2024, doi: 10.3390/batteries10010017.

[16] A. Singh, J. Gupta, and B. Singh, "Design and control of two stage battery charger for low voltage electric vehicle using high gain buck-boost PFC AC-DC converter," in *2022 IEEE 2nd International Conference on Sustainable Energy and Future Electric Transportation (SeFeT)*, Aug. 2022, pp. 1–6. doi: 10.1109/SeFeT55524.2022.9909186.

[17] S. Lacroix, M. Hilairet, and E. Laboure, "Design of a battery-charger controller for electric vehicle based on RST controller," in *2011 IEEE Vehicle Power and Propulsion Conference*, Sep. 2011, pp. 1–6. doi: 10.1109/VPPC.2011.6043189.

[18] D. Benavides, P. Arévalo, E. Villa-Ávila, J. A. Aguado, and F. Jurado, "Predictive power fluctuation mitigation in grid-connected PV systems with rapid response to EV charging stations," *Journal of Energy Storage*, vol. 86, p. 111230, May 2024, doi: 10.1016/j.est.2024.111230.

[19] K. K. Nandini, N. S. Jayalakshmi, and V. K. Jadoun, "A combined approach to evaluate power quality and grid dependency by solar photovoltaic based electric vehicle charging station using hybrid optimization," *Journal of Energy Storage*, vol. 84, p. 110967, Apr. 2024, doi: 10.1016/j.est.2024.110967.

[20] A. Jain and S. Bhullar, "Operating modes of grid integrated PV-solar based electric vehicle charging system- a comprehensive review," *e-Prime - Advances in Electrical Engineering, Electronics and Energy*, vol. 8, 2024, doi: 10.1016/j.prime.2024.100519.
[21] J. Nishanthy, S. Charles Raja, and J. Jeslin Drusila Nesamalar, "Feasibility analysis of solar PV system in presence of EV charging with transactive energy management for a community-based residential system," *Energy Conversion and Management*, vol. 288, p. 117125, Jul. 2023, doi: 10.1016/j.enconman.2023.117125.
[22] F. A. Osman, M. A. R. Eltokhy, A. Y. M. Hashem, and M. Y. M. Hashem, "Grid-connected bidirectional electrical vehicle charger controller parameters optimization using a new hybrid meta-heuristic algorithm," *Journal of Energy Storage*, vol. 95, p. 112307, Aug. 2024, doi: 10.1016/j.est.2024.112307.
[23] K. Zeb, M. Sadiq, W. Uddin, M. M. Gulzar, M. Alqahtani, and M. Khalid, "A Systematic review of topologies, control strategies, challenges, recent developments, and future prospects on emerging electric vehicle chargers," *Energy Strategy Reviews*, vol. 61, p. 101846, Sep. 2025, doi: 10.1016/j.esr.2025.101846.
[24] F. Han, X. Zhang, and M. Li, "Hybrid-mode control for grid-connected inverters and characteristics comparison with current-source mode and voltage-source mode," *International Journal of Electrical Power & Energy Systems*, vol. 170, p. 110911, Sep. 2025, doi: 10.1016/j.ijepes.2025.110911.
[25] S. Islam, S. M. Muyeen, A. Iqbal, F. I. Bakhsh, and L. Ben-Brahim, "Effect of battery storage based electric vehicle chargers on harmonic profile of power system network, current scenario and future scope," *Journal of Energy Storage*, vol. 131, p. 117563, Sep. 2025, doi: 10.1016/j.est.2025.117563.
[26] G. Ramanathan, C. Bharatiraja, H. Kotb, and A. Emara, "PV-assisted modified Z-source inverter for multiport EV charging infrastructure: Access with PV2V," *Energy Reports*, vol. 11, pp. 5716–5732, Jun. 2024, doi: 10.1016/j.egyr.2024.05.036.
[27] I. Ahmed, M. Adnan, and W. Hassan, "A Bidirectional interactive electric vehicles PV grid connected framework for vehicle-to-grid and grid-to-vehicle stability enhancement using hybrid control strategies," *Computers and Electrical Engineering*, vol. 122, p. 109983, Mar. 2025, doi: 10.1016/j.compeleceng.2024.109983.
[28] H. Ahessab, Y. Hakam, A. Gaga, and B. Elhaddadi, "ANN-fuzzy Hybrid Control Strategy for MPPT of Grid-connected PV System with Battery Storage under Fast-changing Atmospheric Condition," *Recent Advances in Electrical & Electronic Engineering (Formerly Recent Patents on Electrical & Electronic Engineering)*, vol. 18, no. 1, pp. 35–49, Jan. 2025, doi: 10.2174/0123520965262688231128053950.
[29] D. V. Bozalakov, S. Qazi, J. D. M. De Kooning, and L. Vandevelde, "Power quality improvement by grid-connected inverters driven by the three-phase damping control strategy operated in different modes," *International Journal of Electrical Power & Energy Systems*, vol. 169, p. 110689, Aug. 2025, doi: 10.1016/j.ijepes.2025.110689.
[30] S. Adak and H. Cangi, "The quality problems at low irradiance in the grid-connected photovoltaic systems," *Electrical Engineering*, vol. 106, no. 5, pp. 6185–6197, Oct. 2024, doi: 10.1007/s00202-024-02351-6.
[31] G. Ramanathan, C. Bharatiraja, H. Kotb, and A. Emara, "PV-assisted modified Z-source inverter for multiport EV charging infrastructure: Access with PV2V," *Energy Reports*, vol. 11, pp. 5716–5732, Jun. 2024, doi: 10.1016/j.egyr.2024.05.036.
[32] F. Barrero-González, M. I. Milanés-Montero, E. González-Romera, E. Romero-Cadaval, and C. Roncero-Clemente, "Control Strategy for Electric Vehicle Charging Station Power Converters with Active Functions," *Energies*, vol. 12, no. 20, p. 3971, Oct. 2019, doi: 10.3390/en12203971.
[33] V. K. Manickam and K. Dhayalini, "Hybrid optimized control of bidirectional off-board electric vehicle battery charger integrated with vehicle-to-grid," *Journal of Energy Storage*, vol. 86, p. 111008, May 2024, doi: 10.1016/j.est.2024.111008.
[34] S. Bind and R. Gupta, "Integration of PV and Wind Energy with Grid and to Charge Electric Vehicles Battery," in *IECON 2023- 49th Annual Conference of the IEEE Industrial Electronics Society*, Oct. 2023, pp. 1–6. doi: 10.1109/IECON51785.2023.10312282.

BIOGRAPHIES OF AUTHORS

Quang-Tho Tran received his M.E. degree in Electrical Engineering from HCM City University of Technology, VNU-HCMC, Vietnam, in 2003, and his Ph.D. degree in Electrical Engineering from HCM-UTE, Vietnam. He is currently working as a lecturer in the Faculty of Electrical and Electronics Engineering, HCM City University of Technology and Engineering. His research interests include electric drives, DC-AC converters, and renewable energy conversion. He can be contacted at email: thotq@hcmute.edu.vn.

Quang-Sang Le was born in Vietnam. He received his engineering degree in technology of electrical and electronics engineering from HCM City University of Technology and Education in 2025, Vietnam. He is currently a master's student in the Faculty of Electrical and Electronics Engineering, HCM City University of Technology and Engineering. His research interests are circuit design, power electronics control, and battery chargers. He can be contacted at email: 2530608@student.hcmute.edu.vn.ss.